LIMNOLOGY and OCEANOGRAPHY

ASLO

Limnol. Oceanogr. 9999, 2023, 1–18

doi: 10.1002/lno.12407

Control of particulate manganese (Mn) cycling in halocline Arctic Ocean waters by putative Mn-oxidizing bacterial dynamics

Manuel Colombo [1*,a], **Julie LaRoche** [2], **Dhwani Desai** [2], **Jingxuan Li** [1,a], **Maria T. Maldonado** [1]

[1]Department of Earth, Ocean, and Atmospheric Sciences, University of British Columbia, British Columbia, Canada
[2]Department of Biology, Dalhousie University, Halifax, Nova Scotia, Canada

Abstract

Particulate Mn, given its high adsorptive capacity and oxidation potential, has profound impacts on the cycling of various trace elements and organic matter in the ocean. Moreover, particulate Mn acts as a sink (via oxidation and adsorption) or as a source (via remineralization and photoreduction) term of bioactive dissolved Mn(II). In the Canadian Arctic Ocean, particulate Mn distributions in the water column revealed the presence of distinctively high particulate Mn concentrations and an overwhelming dominance of the non-lithogenic component to the bulk particulate Mn pool. This phenomenon is of particular importance in halocline waters in the Canada Basin, the Canadian Arctic Archipelago and Baffin Bay, and near-bottom samples in Baffin Bay. Enhanced microbially-mediated Mn oxidation in the water column is suggested as the main mechanism driving the non-lithogenic dominance. Indeed, the microbial community composition data associated with high non-lithogenic particulate Mn (i.e., Mn oxides) display a high relative abundance of taxa (e.g., f.Pirellulaceae, o.Phycisphaerales, f.Cryomorphaceae, g. Moritella) that have been identified in Mn oxide enriched environments. Furthermore, numerous taxa identified in the Canada Basin halocline water, where non-lithogenic particulate Mn peaked, are phylogenetically related to known (cultured) Mn-oxidizing bacteria (MnOB; e.g., Rhodobacteraceae, Oceanospirillaceae, Rhizobiaceae, and other Alphaproteobacteria). Putative MnOB appears to proliferate in certain water masses having a unique set of environmental conditions: low light intensity—alleviating photoinhibition—and high dissolved Mn concentrations, the main drivers known to influence MnOB dynamic, and hence, Mn oxidation.

Manganese (Mn) is an important micronutrient for phytoplankton, as well as prokaryotic microbes, acting as an enzyme co-factor in various intracellular pathways, such as the water-oxidizing complex of photosystem II and the Mn-containing superoxide dismutases (Morel et al. 2013). Given its biological importance, dissolved Mn can limit and/or co-limit (along with iron) biological productivity when this micronutrient is scarce (Middag et al. 2013; Pausch et al. 2019). In addition, authigenic particulate Mn phases as oxides, hydroxides, and oxyhydroxides (i.e., hereafter referred to collectively as Mn oxides) are some of the strongest oxidants in marine waters, modulating the fate of redox-sensitive trace elements and recalcitrant organic matter (Tebo et al. 2004; Hansel 2017). Mn oxides, given their high sorptive capacities, are also strong scavengers, and thus, they regulate the distributions of many particle-reactive trace elements in the ocean (Tebo et al. 2004).

Both particulate and dissolved Mn are delivered to the ocean by means of river discharge (Middag et al. 2011; Colombo et al. 2019*a*), reductive supply from suboxic or anoxic sediments (Vieira et al. 2019; Jensen et al. 2020), atmospheric deposition (Mahowald et al. 2018), sea ice melt (Marsay et al. 2018; Rogalla et al. 2022), and hydrothermal vents (Middag et al. 2011; Fitzsimmons et al. 2017). In the water column, Mn is cycled among its most prevalent oxidation states (II, III, IV) depending on specific environmental conditions (e.g., oxygen levels, pH, microbial community structure), which in turn control their partition between soluble and particulate phases (Tebo et al. 2004). In its reduced

*Correspondence: manuel.colombo@alumni.ubc.ca

Additional Supporting Information may be found in the online version of this article.

[a]Present address: Department of Marine Chemistry and Geochemistry, Woods Hole Oceanographic Institution, Woods Hole, Massachusetts, USA

Author Contribution Statement: Conceptualization: M.C. and M.T.M. Formal analysis: M.C., J.L.R., and D.D. Funding acquisition: M.T.M. and J.L. Methodology: M.C., J.L., J.L.R., and D.D. Visualization: M.C., J.L.R., and D.D. Writing—original draft: M.C. and M.T.M. Writing—review and editing: J.L.R., D.D., and J.L.

state, thermodynamically favored under low pH and oxidation potential conditions, Mn(II) is mostly soluble (dissolved Mn) and bioavailable, whereas the oxidized species Mn(III, IV) are insoluble, constituting a large fraction of the particulate Mn pool in oceanic waters (Tebo et al. 2004, 2010; Lam et al. 2018; Xiang and Lam 2020). The trivalent Mn species are not stable, disproportionating rapidly to Mn(II) and Mn(IV); however, recent studies have reported the presence of organic ligands stabilizing and solubilizing Mn(III) (Oldham et al. 2017; Wright et al. 2018). Moreover, inorganic transient stabilization of Mn(III) by pyrophosphate complexation has been described in laboratory experiments and inferred in field studies (Webb et al. 2005; Pakhomova et al. 2009). Abiotic oxidation of Mn is favored in most oceanic waters, nonetheless, this reaction has an extremely low kinetic rate, compared to biologically-mediated oxidation, and hence, microbes (bacteria and fungi) are considered the most important drivers of Mn oxidation and precipitation in aquatic environments (Cowen and Silver 1984; Dick et al. 2006; Hansel 2017).

Bacteria with Mn-oxidizing ability are phylogenetically diverse and environmentally widespread, and their activity has been described in a wide range of environments (freshwater, seawater, sediments, and soils; *see* Hansel 2017 and references therein). Bacterial Mn oxidation is carried out directly by multicopper oxidases and heme peroxidases, or indirectly through the enzymatic generation of extracellular superoxide radicals (Hansel 2017). Manganese oxidation reactions are energetically favorable, and hence, Mn-oxidizing bacteria (MnOB) could potentially benefit directly from these reactions as an energy source. Indeed, a recent laboratory study has demonstrated that Mn(II) oxidation drives lithotrophic energy metabolism and growth in a co-culture of two microbial species, as they couple extracellular Mn oxidation to aerobic energy conservation and autotrophic CO_2 fixation (Yu and Leadbetter 2020). In addition, MnOB could also benefit from the ability of manganese oxides to promote the degradation of a wide range of complex organics (i.e., refractory organic matter, humic, etc.), the scavenging of essential trace elements, and by gaining protection from toxic heavy metals, predation, and oxidative damage by the Mn oxides coatings (Tebo et al. 2004, 2010, and references therein).

Considering the importance of particulate Mn in modulating the cycling of other trace elements and organic matter, and the fact that particulate Mn is a source/sink component of bioavailable Mn(II), the study of particulate Mn concentrations and factors controlling its distribution in the ocean is a key endeavor of international research programs such as GEOTRACES. In recent years, great advances have been made mapping particulate Mn distribution in all major ocean basins and investigating its biogeochemical cycle (Lee et al. 2018; Xiang and Lam 2020; GEOTRACES Intermediate Data Product Group 2021). Overall, particulate Mn concentrations are generally at picomolar levels, with the lowest concentrations usually at the surface, due to the combined effect of photoreductive dissolution of Mn oxides and photo-inhibition of MnOB (Lam et al. 2015, 2018; van Hulten et al. 2017). This relatively uniform and low background particulate Mn distribution is interrupted by particulate Mn hotspots, associated with, for example, hydrothermal inputs, lithogenic particles (riverine and sediment resuspension), and redox cycling above reducing sediment (Lam et al. 2015; Fitzsimmons et al. 2017; Morton et al. 2019). Among oceanographic regions where particulate Mn data are available, the Canadian Arctic Ocean displayed considerably high Mn oxide concentrations, with sharp peaks along halocline waters (Xiang and Lam 2020; Colombo et al. 2022). Geochemical data, along with timescale analysis of halocline water circulation, suggested that the high particulate Mn feature in the winter Bering Sea Water in the Canada Basin and in the Arctic Water in Baffin Bay are related to enhanced bacterially-mediated Mn oxide precipitation within the water column (Colombo et al. 2022). These subsurface halocline waters (winter Bering Sea Water and Arctic Water) have the potential to carry large amounts of Mn oxides, given their distinctive environmental conditions (i.e., low light and elevated dissolved Mn concentrations advected from shallow shelves) and the entrainment of sedimentary MnOB (i.e., due to their close interaction with the seafloor; Colombo et al. 2022).

However, microbial community composition data are still lacking to elucidate the role of MnOB in driving particulate Mn distribution in the Canadian Arctic Ocean. This study integrates recently published particulate Mn data from the deep Canadian Arctic Ocean basins (Colombo et al. 2022) and the Canadian Arctic Archipelago (Colombo et al. 2021) with new data on the genetic diversity of these microbial communities aiming to understand the integral cycle of particulate Mn in the Canadian Arctic Ocean. The mechanisms by which halocline waters are enriched in non-lithogenic particulate Mn and the key environmental factors correlated with MnOB community composition, and consequently Mn oxides distribution, are also discussed.

Methods

Particulate trace element sampling and analysis

Vertical profiles of particulate Mn were collected at 17 stations during the 2015 Canadian GEOTRACES Arctic Expedition (10 July 2015 to 01 October 2015) on board CCGS Amundsen (Fig. 1). Four basins were sampled in this expedition including the Canada Basin (Stas. CB2, CB3, and CB4), the Canadian Arctic Archipelago (Stas. CB1, CAA1, CAA3–CAA9), Baffin Bay (Stas. BB1–BB3), and the Labrador Sea (Stas. LS2 and K1). The sampling and analytical procedures of particulate Mn analyses are fully described in Colombo et al. (2022). In brief, a trace metal clean sampling system equipped with twelve 12 L Teflon-coated GO-FLO bottles (General Oceanics) was employed to collect seawater samples for particulate Mn and other trace element elements. The GO-FLO bottles were then transferred to a portable trace metal clean sampling van,

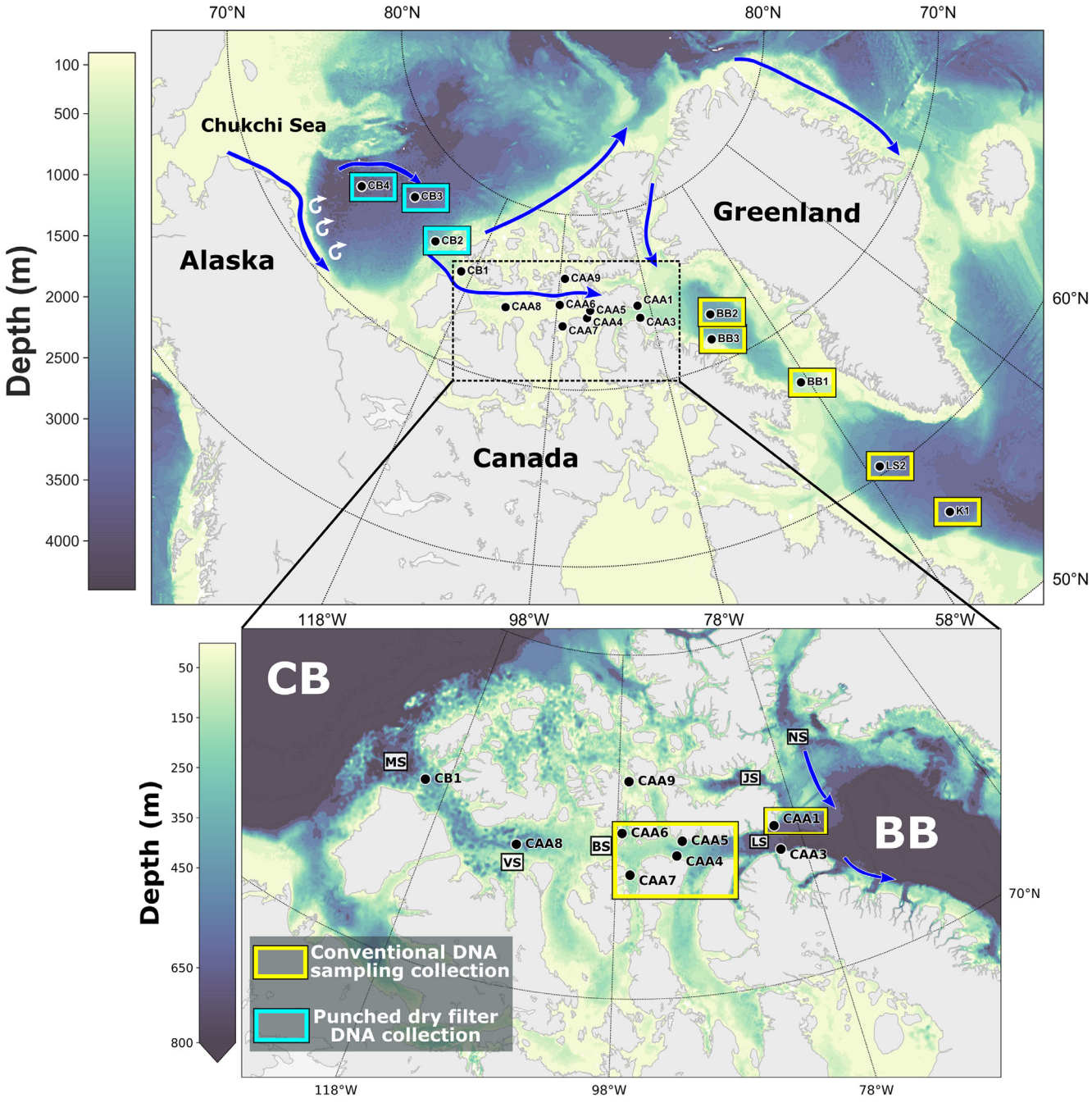

Fig. 1. Stations sampled for particulate Mn and DNA during the Canadian Arctic GEOTRACES cruises (GN02 and GN03), alongside bathymetry and a schematic of halocline Arctic water circulation (blue arrow; after Aksenov et al. 2011; Kondo et al. 2016). DNA sample collection was performed following standard procedures (yellow/black-edged rectangles) and from punches from dry filters (cyan-blue/black-edged rectangles). For details regarding DNA sampling collection, please refer to the Methods section. Canada Basin stations: CB2–CB4, Canadian Arctic Archipelago stations: CB1 and CAA1–CAA9, Baffin Bay stations: BB1–BB3, Labrador Sea stations: LS2 and K1. Landmarks and straits of the Canadian Arctic Archipelago are displayed in the inset; MS: M'Clure Strait, VS: Viscount Melville Sound, BS: Barrow Strait, LS: Lancaster Sound NS: Nares Strait, JS: Jones Sound. Parry Channel is the main pathway in the central Canadian Arctic Archipelago, connecting M'Clure Strait with Lancaster Sound.

where the seawater was collected into LDPE cubitainers (Bel-Art and Nalgene), followed by the filtration step, which was carried out inside a HEPA-filtered clean air bubble, using a 0.45 μm, 47 mm diameter Supor filter (Pall). The free-living microbial community ($\sim$ 0.5–1 μm), besides particle-associated microbes, are most probably collected with the filter pore size (0.45 μm) employed for particulate Mn sampling (Cowen and Silver 1984; Kellogg and Deming 2009). After filtration, the

filters were dried and stored in poly bags until further particulate trace element analysis. Containers and apparatus were cleaned according to GEOTRACES protocols.

At the University of British Columbia (UBC), the dry filters were completely digested in class 1000 laboratories and under class 100 laminar flow fume hoods following the protocol described by Ohnemus et al. (2014). All the plasticware used during filter digestion and sample preparation was cleaned according to GEOTRACES protocols. Filters were placed in 15 mL Teflon vials (Savillex) and then digested in a heated (110°C; 60–120 min) Teflon block using a mixture of concentrated sulfuric acid (1.2 mL H_2SO_4) and hydrogen peroxide (0.4 mL H_2O_2) to completely dissolve the organic fraction and the Supor filters. The vials were then placed in the Teflon block and the solution was dried at 245°C. The remaining materials were digested (110°C) for 4 h using a concentrated acid mixture of nitric acid–hydrochloric acid–hydrofluoric acid (HNO_3, HCl, and HF), and then taken to dryness. All reagents used in the digestion and subsequent sample preparation, including the four acids and H_2O_2, were Optima grade (Fisher Scientific). Final pellets were resuspended in 1% HNO_3 spiked with 10 ppb Indium, as an internal standard. The samples were diluted and then analyzed in the Pacific Centre for Isotopic and Geochemical Research at UBC, using a high-resolution Thermo Finnigan Element2 ICP-MS. A medium mass resolution was selected for Mn to remove isobaric interferences. The quantification was achieved from a 12-point calibration curve prepared in 1% trace metal grade HNO_3 with 10 ppb Indium. This method yielded a filter blank concentration (Supor 0.45 μm; $n = 3$) of 48 ± 1.4 pmol filter^{-1} and an accuracy, calculated by analyzing the BCR 414 certified reference material ($n = 4$), of 97%. The relative standard deviation (1RSD) was 14%. In addition, results from GEOTRACES inter-comparison exercise, including flow through blank filters, particulate samples collected at 45 m at the SAFe station and at 130 m in the Santa Barbara Basin, are presented in Supporting Information Table S1.

Non-lithogenic particulate Mn (i.e., excess of particulate Mn over lithogenic sources) was estimated as total particulate $\mathrm{Mn} - \left[\text{total particulate Mn} \times \left(\frac{\text{particulate Al}}{\text{particulate Mn}}\right)_{\text{sample}} \times \left(\frac{\text{particulate Mn}}{\text{particulate Al}}\right)_{\text{UCC}}\right]$, where $\left(\frac{\text{particulate Mn}}{\text{particulate Al}}\right)_{\text{UCC}}$ is the upper continental crust ratio retrieved from Rudnick and Gao (2013) and particulate Al concentration data from the samples was retrieved from Colombo et al. (2021, 2022); estimated negative non-lithogenic values were set to 0.

Environmental DNA samples

Environmental DNA sample collection

DNA material was sampled from water collected, using a regular rosette equipped with Niskin bottles, in the Labrador Sea (LS2, K1), Baffin Bay (BB1–BB3), and the Canadian Arctic Archipelago (CAA1, CAA4–CAA7), during the same sampling event as that of particulate trace elements (Fig. 1), and at depths matching particulate Mn samples. Immediately after collection, four liters of seawater were filtered through in-line 47 mm polycarbonate filters of 3-μm pore size, using a peristaltic pump. The filters were placed in screwcap microcentrifuge tubes and immediately stored at −80°C until processed in LaRoche's laboratory at Dalhousie University. Given sampling constraints, the three DNA samples from the Canada Basin were not collected as described above, but instead, they were obtained from punches of three dry filters (0.8 μm, 142 mm diameter polyethersulfone membrane filters, dried at ~ 60°C for 48 h on board), obtained from large volume water filtration with MacLane pumps (courtesy of Dr. Diana Varela, Univ. of Victoria) at depths matching the particulate Mn peak in winter Bering Sea Water (Sta. CB2: 140 m; CB3: 180 m; CB4: 220 m).

All DNA samples (i.e., from the Labrador Sea, Baffin Bay, the Canadian Arctic Archipelago, and the Canada Basin) were extracted with Qiagen DNAeasy extraction kits according to the protocol provided by the supplier, and as previously described by Zorz et al. (2019). DNA concentrations were measured with a Nanodrop instrument and the DNA sample was aliquoted for Illumina DNA sequencing of the V4-V5 variable region of the 16S rRNA gene (Parada et al. 2016).

16S rRNA gene amplicon sequencing and statistical analysis

Highly multiplexed V4-V5 16S rRNA variable regions read were processed using the Amplicon sequencing Standard Operating Procedure following the Microbiome Helper workflow and scripts (https://github.com/LangilleLab/microbiome_helper/wiki/16S-Bacteria-and-Archaea-Standard-Operating-Procedure; Comeau et al. 2017). In summary, paired-end Illumina reads were stitched together using the program Pear (Zhang et al. 2014) and filtered by quality score and length using the FastX software suite (http://hannonlab.cshl.edu/fastx_toolkit/). Chimeric sequences were removed using Vsearch (Rognes et al. 2016). The cleaned and filtered reads were then clustered into Operational Taxonomic Units (OTUs) using the pick_open_reference_otus.py script from QIIME (Caporaso et al. 2010), by comparing them against the GreenGenes 16S rRNA database (DeSantis et al. 2006) at an identity threshold of 97%. The OTUs were filtered to remove OTUs that occurred in less than 15 samples (minimum occurrence) or OTUs that had less than 0.01% of the total reads, resulting in a total of 737 OTUs from 66 DNA samples for which particulate Mn data were available. The three DNA samples from the Canada Basin extracted from dry filters were processed similarly through the pipeline, however, they were not included in the correlation analysis between particulate Mn and microbial community structure nor in the bidirectional hierarchical clustering analysis, because the filter type, pore size, and sample collection were different.

Correlation network construction. The OTU counts and the particulate Mn measurements for the 66 samples were used to generate a correlation network using four different metrics (Spearman's correlation, Pearson's correlation, Bray–

Curtis distance, and Kullback–Leibler distance) by the plugin CoNet (Faust and Raes 2016) in the program Cytoscape (Shannon et al. 2003). From this network, 66 OTUs that were correlated (both positive and negative) with particulate Mn concentrations were further analyzed for their occurrence patterns.

Non-parametric statistical analysis. Based on a bidirectional hierarchical clustering of the particulate Mn-associated OTUs, the samples were divided into two groups designated as HighMn and LowMn, based on the mean particulate Mn concentrations in these groups. The non-parametric multivariate test for analysis of similarity (ANOSIM) was used to investigate whether the microbial community composition (distribution of OTUs) in the HighMn and LowMn groups were significantly different, and then, the Simper routine was employed to identify the discriminating OTUs between these groups. These analyses were performed using the program PrimerE v6 (Clarke and Gorley 2006). All additional analyses and plotting were done using R and Python 3.6.0. programming languages.

Results and discussion

The novel genomic and microbial community structure dataset (OTUs relative abundance distributions) from the Canadian Arctic Ocean (Research Data Electronic Annex, Supporting Information Tables SRD1–SRD4) presented in this study, together with particulate Mn data (Supporting Information Table SRD5), retrieved from Colombo et al. (2021, 2022), further expands our knowledge on the potential role of MnOB in modulating the cycling of Mn in the Canadian Arctic Ocean.

Particulate manganese distributions and composition across the Canadian Arctic Ocean

Distributions of total particulate Mn in the deep Canada Basin (Stas. CB2, CB3, and CB4) and Baffin Bay (Stas. BB1, BB2, and BB3) shared similar features. The lowest concentrations (Canada Basin: 418 ± 259 pmol L^{-1} and Baffin Bay: 460 ± 139 pmol L^{-1}) were measured in the upper 25 m (i.e., Canada Basin $\sigma_\theta < 23.5$; Baffin Bay $\sigma_\theta < 26.3$), where particulate Mn represent only 1.7–19.6% of the total Mn pool (particulate + dissolved Mn; Fig. 2). Below surface waters, total particulate Mn concentrations sharply increased within halocline waters, both in the winter Bering Sea Water in the Canada Basin ($z = \sim$ 100–300 m and $\sigma_\theta = 25.9$–27.1) and in the Arctic Water in Baffin Bay ($z = \sim$40–180 m and $\sigma_\theta = 26.3$–27.1), reaching concentrations as high as 5127 and 2083 pmol L^{-1}, respectively (Fig. 2). Interestingly, along with the particulate Mn peak, there is a rapid shift of the Mn pool dominant fraction, with particulate Mn accounting for 51.2–74.1% of the total Mn (particulate + dissolved Mn) in the winter Bering Sea Water and 30.8–58.5% in Arctic Water (Baffin Bay; Fig. 2). Although the particulate Mn fraction was still the dominant phase (particulate Mn = 51.9–93.2% of total Mn; Fig. 2) in the Canada Basin and Baffin Bay deep waters ($\sigma_\theta > 27.1$), total particulate Mn concentrations were lower than those in the halocline waters. In Baffin Bay, total particulate Mn concentrations peaked in near-bottom waters, particularly at Stas. BB3 and BB1 (4849 and 10,818 pmol L^{-1}, respectively; Fig. 2). An overwhelming dominance of non-lithogenic particulate Mn (i.e., not derived from crustal weathering) is another notable feature observed in the Canada Basin and Baffin Bay (Fig. 2), especially in the winter Bering Sea Water (> 97% of total particulate Mn) and Arctic Water in Baffin Bay (> 90%). This excess of particulate Mn over the lithogenic component is attributed to microbially-mediated authigenic Mn(III, IV) oxide formation in slope regions and the ocean interior (Colombo et al. 2022).

The Canadian Arctic Archipelago (Stas. CB1, CAA1, and CAA3–CAA9) is a dynamic environment where sediment resuspension events, river water inputs, glaciers, and glacially-fed streams are ubiquitous, exerting an important control on trace metal geochemistry (Colombo et al. 2019*a*, 2020). As such, total particulate Mn concentrations in the Canadian Arctic Archipelago reflect the heterogeneity of sources and processes in this region. In the tranquil western Canadian Arctic Archipelago (Stas. CB1 and CAA8), total particulate Mn profiles resemble those of inflowing Canada Basin waters, though with diminished concentrations, exhibiting a dominance of the particulate phase with increasing depth below surface waters, and no benthic enrichment (Fig. 2). Unlike western CAA, the stations located east of Barrow Strait, where sediment resuspension and dissolved Mn concentrations are significantly higher (Colombo et al. 2020, 2021), displayed a clear benthic enrichment signature, with total particulate Mn concentrations increasing rapidly with depth below $\sim$ 50 m ($\sigma_\theta > 25.5$; Fig. 2). However, the non-lithogenic particulate Mn component of the stations located in Penny Strait (Sta. CAA9), Barrow Strait (Sta. CAA6), and northern Lancaster Sound (Sta. CAA1, close to Devon glaciers) is negligible (i.e., lithogenic dominated), and contrast with the other stations located east of Barrow Strait (Stas. CAA4, CAA5, CAA7, and CAA3), where non-lithogenic particulate Mn concentrations are greater (Fig. 2). This difference is attributed to sediment-laden meltwater runoff and subglacial discharges from Devon glaciers, impacting specially the Sta. CAA1, delivering lithogenic-derived particles (Colombo et al. 2019*b*, 2021), and enhancing water column mixing at the Stas. CAA1, CAA6, and CAA9.

In the Labrador Sea (Stas. K1 and LS2), vertical profiles of total particulate Mn exhibited the same general trends, namely a surface minimum and a progressive increase with depth (Fig. 2). However, particulate Mn distributions in the Labrador Sea revealed unique features among the studied Canadian Arctic Ocean basins, such as recording the lowest concentrations ($\sim$ 1 order of magnitude lower), reduced particulate phase dominance (< 38% of total Mn) and balanced particulate Mn contributions (i.e., non-lithogenic source $\sim$ lithogenic source; Fig. 2).

Overall, the non-lithogenic component shapes the distribution of particulate Mn in both the deep basins (to a lesser extent for the Labrador Sea) and the shallow Canadian Arctic Archipelago. Halocline waters, such as the winter Bering

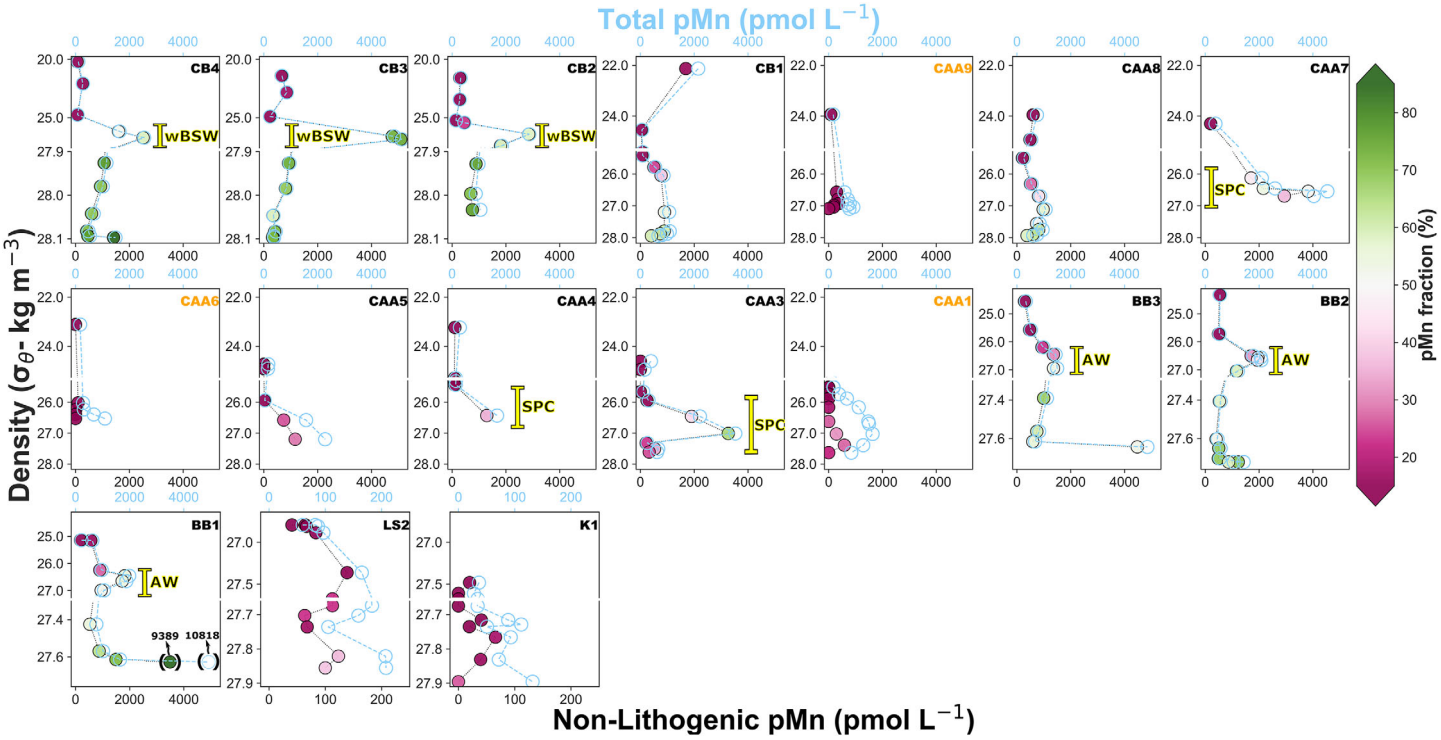

Fig. 2. Profiles of non-lithogenic particulate Mn (filled symbols) and total particulate Mn (pMn; filter pore size: 0.45 μm) vs. potential density (σ_θ) in the Canadian Arctic Ocean across the Canada Basin (CB2–CB4), the western Canadian Arctic Archipelago (CB1 and CAA8), Northern Parry Channel (CAA1, CAA5), Barrow Strait (CAA6), Southern Parry Channel (CAA3, CAA4, and CAA7), Penny Strait (CAA9), Baffin Bay (BB1–BB3), and the Labrador Sea (LS2 and K1). As the deepest samples from the BB1 station had extremely high concentrations of Mn, these values are shown between parentheses to emphasize the features of the rest of the profile. The particulate Mn fraction (% of total Mn $= \frac{\text{total pMn}}{(\text{total pMn}+\text{dMn})}$) of each sample, indicated with the color scale bar, was calculated using dissolved Mn (dMn; filter pore size: 0.2 μm) data from Colombo et al. (2020). Stas. CAA1, CAA6, and CAA9, highlighted in orange, displayed lower total particulate Mn concentrations and reduced non-lithogenic sources. Water masses with elevated non-lithogenic particulate Mn concentrations and high relative abundance of putative MnOB, such as winter Bering Sea Water (wBSW), Southern Parry Channel subsurface waters (SPC), and Arctic Water (AW) are identified in the figure.

Sea Water, the Arctic Water, and Southern Parry Channel subsurface waters together with near-bottom waters in Baffin Bay have the highest non-lithogenic particulate Mn concentrations (Fig. 2). This phenomenon could be related to enhanced bacterially-mediated Mn(III/IV) oxide formation in these waters, which—given their unique environmental conditions—have the potential to promote a significant increase of MnOB. Other sources of non-lithogenic particulate Mn such as phytoplankton-derived export and/or advective transport of sedimentary Mn oxides from adjacent shelf settings are not significant. Enhanced primary production at the surface and associated export of phytoplankton detritus could be linked to higher contributions of non-lithogenic particulate Mn in the seawater (Twining et al. 2015); nonetheless, this is not a substantial source in the Canadian Arctic Ocean. Non-lithogenic particulate Mn fractions are relatively similar across the Canada Basin and Baffin Bay (Fig. 2), despite the large differences in export production between these two deep basins, with much lower primary productivity rates in the Canada Basin compared with Baffin Bay (Hill et al. 2013; Varela et al. 2013). Moreover, the lowest non-lithogenic contributions were measured in the Labrador Sea (Fig. 2), where intense phytoplankton spring blooms took place before sampling (Colombo et al. 2022).

Advective sedimentary Mn oxide inputs from the Chukchi and the Canadian Arctic Archipelago shelve sediments—as mediated by the reduction of Mn in the sediment, follow by diffusion to overlying waters, where redox-sensitive Mn is then precipitated—are also not driving Mn distributions in the Canadian Arctic Ocean. In the Chukchi Shelf, large pulses of organic matter trigger strong reducing conditions in sediments, which in turn promote large upward fluxes of reduced dissolved Mn(II) from sediments into the overlying seawater (Granger et al. 2018; Vieira et al. 2019). However, due to its slow oxidation kinetics and potential photoinhibition of MnOB in the shallow Chukchi shelves (< 50 m), most of the Mn in the winter Bering Sea Water remains in the dissolved phase during across-shelf transport, leaving Chukchi shelf waters virtually depleted of Mn oxides and highly enriched in dissolved Mn (Jensen et al. 2020; Xiang and Lam 2020). In the shallow Canadian Arctic Archipelago shelves, the lower pulses of organic matter, compared with the Chukchi Shelf, and

the strong mixing regimes do not favor reductive benthic conditions, and thus, sedimentary supply of reduced Mn(II) is not anticipated to be significant (Colombo et al. 2021; Lehmann et al. 2022). Therefore, the excess of particulate Mn over continental crust values across the Canadian Arctic Ocean, and especially in halocline waters, is most likely explained by the authigenic formation of Mn(III/IV) oxides in the water column. The microbial community analysis presented in this study adds new evidence for the bacterially-mediated authigenic Mn oxidation argument across the Canadian Arctic, demonstrating that the highest non-lithogenic particulate Mn (hereafter referred to as Mn oxides) features are associated with a high relative abundance of (cultured) taxa known to have the ability to oxidize Mn.

Microbial community structure associated with particulate manganese

Microbial communities in the Labrador Sea, Baffin Bay, and the Canadian Arctic Archipelago

Given the dominance of Mn oxides in most of the Canadian Arctic Ocean samples and the role of MnOB as catalyzers of Mn(II) oxidation (Moffett 1997; Lee et al. 2018; Wright et al. 2018; Morton et al. 2019), we investigated the microbial community composition from 66 paired DNA and particulate Mn samples collected in the Labrador Sea, Baffin Bay and the Canadian Arctic Archipelago, during the August 2015 Canadian GEOTRACES Arctic Expedition (cruise ArcticNet 1502). OTUs were determined from the 16S rRNA gene amplicon sequence reads. Note that the samples from the Canada Basin were collected on a following cruise (ArcticNet 1503) a month later (September 2015) using different protocols (*see* Methods section). Thus, the results from the Canada Basin samples are presented in a separate subsection below.

Within the 66 samples for which paired chemical and DNA analyses were available, 737 OTUs (Supporting Information Table SRD1) were found to be both prevalent (occurring in at least 15 samples) and abundant (contributing to at least 0.01% of the total reads). We investigated the correlation network between the amplicon sequence counts of these 737 OTUs and total particulate Mn concentrations and determined that 66 of the 737 OTUs were significantly, positively or negatively, correlated ($p < 0.05$) with total particulate Mn (Supporting Information Fig. S1; Supporting Information Table SRD2). The relative abundance of these 66 particulate Mn-correlated OTUs, and their taxonomic affiliations, are shown in Supporting Information Fig. S2. We performed bidirectional hierarchical clustering of these 66 OTUs based on their relative abundance patterns in our samples. Hierarchical clustering methodology is a powerful data mining approach for the first exploration of "omic" data. Here, it enabled samples to be grouped blindly according to the relative abundance profiles of the 66 OTUs. The bidirectional hierarchical clustering returned two major sample clusters (Fig. 3). The median total particulate Mn concentrations of the samples comprising the two clusters were significantly different, and thus they were designated as LowMn and HighMn groups (median particulate Mn concentrations in the HighMn group: 1436.8 pmol L^{-1}, $n = 35$ and LowMn group: 219 pmol L^{-1}, $n = 31$; Welch's t-test $p = 0.0004$; Fig. S3).

The bidirectional hierarchical clustering (Fig. 3) revealed that the OTUs associated with the HighMn sample group belonged to several phyla, including Bacteroidota (i.e., within the Cryomorphaceae, Saprospiraceae, and Fluviicola families, and the particle-associated NS9 clade), Planctomycetota (the agg27 clade, as well as members of the OM190 clade, such as CL500-15), Verrucomicrobiota (e.g., the Arctic97B-4 clade), Proteobacteria (i.e., within the Gammaproteobacteria class, the Colwelliaceae, Piscirickettsiaceae, and Moritellaceae families; and within the Deltaproteobacteria class, the OM60 clade), and OTUs associated with the phyla Nitrospinota and the ammonia-oxidizing Thaumarchaeota (e.g., Nitrosopumilaceae family; Fig. 3). Some of the microbial phylogenetic groups identified within the HighMn sample group (i.e., Arctic 97B-4, Colwelliaceae, Nitrosopumilaceae, Phycisphaerae, and Nitrospinae) have been found associated with Fe–Mn crust environments and biofilms (Kato et al. 2017; Bergo et al. 2021).

The similarity between microbial communities in the 66 samples was further assessed using the NMDS ordination of the Bray–Curtis dissimilarity index, which compares the beta-diversity of the microbial community composition (i.e., distance of their OTUs occurrence profiles). This index, based on the log-transformed relative abundances of the original 737 taxa, also revealed a clear separation between the microbial communities associated with the HighMn group (subsurface and deep waters) and LowMn group (surface waters; Supporting Information Fig. S4). This was further confirmed by an ANOSIM test on the OTU distributions in the two groups, which showed a Global R value of 0.877 with a significance of 0.1% (Supporting Information Fig. S4).

A SIMPER routine analysis (including the original 737 OTUs) was then used to independently identify the discriminating OTUs between the LowMn and HighMn sample groups (Supporting Information Table S2). The average dissimilarity of the relative abundance of an OTU between the HighMn and LowMn groups, divided by the standard deviation for the OTU in samples of either group, reflects the discriminating power of a specific OTU (i.e., the best OTUs discriminators have the highest ratio). Fifteen of 30 most discriminating OTUs for the HighMn group belong to the phylum Planctomycetes, and more specifically to the Pirellulaceae and Phycisphaerae families, as well as the agg27 clade, and members of the uncultured OM190 (i.e., CL500-15). Indeed, an OTU of the OM190 clade (GT15 Reference OTU1-c-OM190) was the most discriminating OTUs between LowMn and HighMn groupings (Supporting Information Table S2). The remaining 15 of the 30 most discriminating OTUs belong to the phyla Verrucomicrobiae (e.g., Arctic97B-4 clade), Bacteroidetes (Saprospiraceae and Cryomorphaceae families), and Proteobacteria (within the

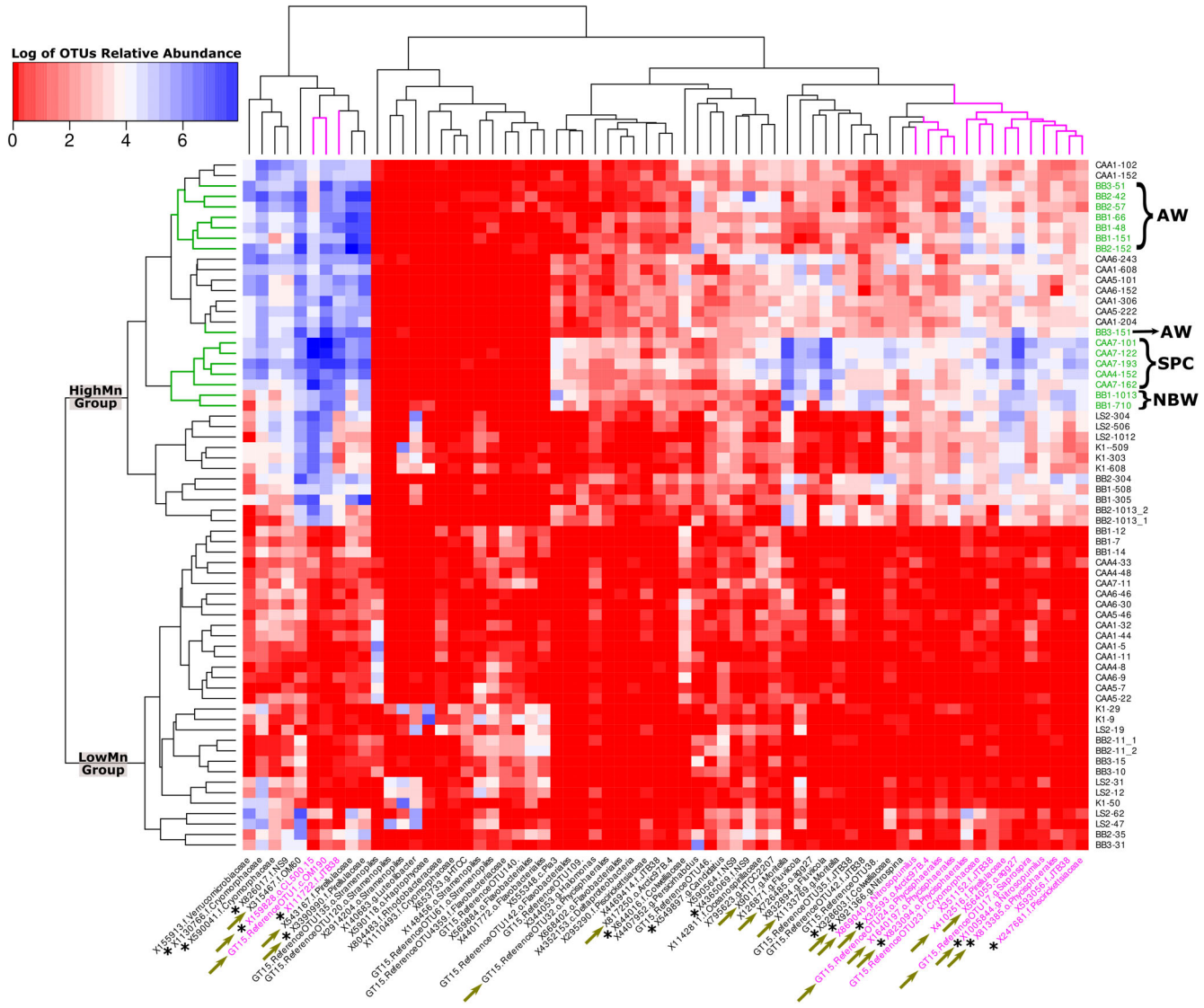

Fig. 3. Two-way unsupervised hierarchical clustering of the samples (from the Canadian Arctic Archipelago, Baffin Bay, and the Labrador Sea) and taxa based on the log-relative abundance profiles for the 66 Mn-associated OTUs. The full taxonomy of the 66 OTUs is found in Supporting Information Table SRD4. The median total particulate Mn concentrations in the two clusters of samples (LowMn: 219 pmol L^{-1} and HighMn: 1436.8 pmol L^{-1}) were calculated and are presented as box and whisker plots in Supporting Information Fig. S3. Sample names on the right-hand side are labeled with the station name as in Fig. 1, and the depth of sample collection at that station. Samples collected at depths corresponding to subsurface Arctic Water in Baffin Bay (AW), Southern Parry Channel subsurface waters (SPC), and near-bottom waters in Baffin Bay (NBW) are in green text (name of station on the right and clades on the left). Discriminating OTUs between LowMn and HighMn groupings (Simper analysis; Supporting Information Table S2) are in magenta text (name of OTUs on the bottom and clades on the top), taxa related to microbial groups closely associated with Mn oxide enriched environments are indicated with olive green arrows (refer to Table 1 for more information), and OTUs which were identified in both samples collected in the Winter Bering Sea Water (wBSW) in the Canada Basin, where Mn oxides peaked, and in the Canadian Arctic Archipelago, Baffin Bay, and the Labrador Sea are indicated by an asterisk (*).

gammaproteobacteria class, the Piscirickettsiaceae family; and within the deltaproteobacteria class, the OTU60 clade). Furthermore, Nitrospina within the Nitrospinota phylum, and the Nitrosopumilaceae family of aerobic ammonium-oxidizer crenarchaea within the phylum Thaumarcheota, were also good discriminators between the HighMn and LowMn grouping, coming within the top 30 discriminating OTUs.

Bacterial chemolithoautotrophy via manganese oxidation has been recently demonstrated in enrichment co-cultures of *Ramlibacter lithotrophicus* (a betaproteobacterium) and *Candidatus Manganitrophus noduliformans* (distantly related to *Nitrospira* and *Leptospirillum*, in the Nitrospirota phylum; Yu and Leadbetter 2020). However, many of the known (cultured) Mn(II) oxidizing microbes are also heterotrophs (Ehrlich and

Newman 2008; Tebo et al. 2010) and are extremely diverse phylogenetically with members identified in Alphaproteobacteria, Gammaproteobacteria, Betaproteobacteria, Actinobacteria, Bacteroidetes, Firmicutes (Hansel 2017). In this field study, we cannot specifically identify which members of the microbial community associated with the HighMn group might be responsible for Mn oxidation; however, several characteristics of the HighMn group microbial community are noticeable. First, as expected by the filter pore size used for these environmental DNA samples (3 μm), numerous OTUs identified here (e.g., NS9, CL500-15, agg27, etc.; Fig. 3) are known to be particle-associated (DeLong et al. 1993; Fuchsman et al. 2012; Zhang et al. 2013; Milici et al. 2017); given the filter size, these particle-associated microbial communities are anticipated to be enriched over small and free-living microbes. Notwithstanding, particle clogging during filtration reduces the effective filter pore size over time, certainly collecting some free-living microbes too. Second, a third of the most discriminating and abundant OTUs belongs to the Phycisphaerae family and the OM190 clade—both within the Planctomycetes phylum—which have been proposed to play a role in anammox pathway and possibly Mn oxidation in the deep-sea Fe hydroxide deposits associated with diffuse venting (rich in dissolved Fe and Mn) from Arctic Mid Ocean Ridge (Storesund and Øvreås 2013). Third, several studies linking Mn oxidation to ammonia oxidation (Luther et al. 1997; Storesund and Øvreås 2013; Wang et al. 2021) support the findings in our study of the Canadian Arctic Ocean that the top three discriminating OTUs associated with HighMn samples belong to the Pirellulacea family and Phycisphaerales order, as these taxa include ammonia-oxidizing bacteria often found in marine sponges and deep-sea corals (Mohamed et al. 2010; Kellogg et al. 2016). In addition, chemolithoautotrophic nitrite/nitrate or ammonia-oxidizing microbes, from the Nitrospinae and Nitrospumilaceae families, respectively, are often associated with Fe–Mn crust environments (Bergo et al. 2021), and were found in the top 30 discriminating OTUs in our study (Supporting Information Table S2). Likewise, several discriminating OTUs belonging to the phyla Planctomycetes (e.g., Pirellulaceae), Gammaproteobacteria, and Bacteroidetes (e.g., Saprospiracea) are abundant in nitrifying microbial consortia associated with biological Mn(II) oxidation in wastewater bioreactors and thrive in high dissolved Mn and low organic carbon conditions (Cao et al. 2015). These combined findings suggest that ammonia-oxidizing microbes, nitrifiers, and MnOB might be closely associated in these environments and that the Mn and N cycles might be linked.

Microbial communities in the Canada Basin

Due to sampling constraints (*see* Methods section), frozen DNA samples were not collected in the Canada Basin. Nonetheless, we explored the microbial community associated with the subsurface particulate Mn peak in the winter Bering Sea Water in the Canada Basin through the analysis of DNA extracted from dried membrane filters (0.8 μm) at Stas. CB2, CB3, and CB4. The samples from these stations were processed as for the other samples with amplification of the V4-V5 variable region of the 16S rRNA gene, and with the same bioinformatic pipeline as described in the Methods section. Thus, the microbial community data from the winter Bering Sea Water in the Canada Basin can be compared to the rest of the Canadian Arctic Ocean. In the winter Bering Sea Water, where the Mn oxide peak was observed (Fig. 2), members belonging to the Planctomycetota (e.g., Phycisphaerae and Planctomycetes), Acidobacteria (e.g., Acidobacteria and Solibacters), Proteobacteria (e.g., alphaproteobacteria, gammaproteobacteria, betaproteobacteria, and deltaproteobacteria), Bacteroidota (e.g., Flavobacteria and Saprospirae), and Verrucomicrobiota phyla also dominated the microbial communities (Fig. 4; Supporting Information Table SRD4).

To reconcile the two microbial community datasets, from the Canada Basin and the remaining Canadian Arctic Ocean stations, we constructed a phylogenetic tree (Supporting Information Fig. S5) that encompasses the positive Mn-correlated OTUs from samples collected in the Canadian Arctic Archipelago, Baffin Bay, and the Labrador Sea (Fig. 3), as well as the OTUs obtained from the Canada Basin samples (Fig. 4; Supporting Information Table SRD4). In addition, 26 Mn-oxidizing microbes highlighted in Hansel (2017) as representative MnOB were used to construct this maximum likelihood phylogenetic tree. Interestingly, several OTUs (e.g., Rhodobacteraceae, Oceanospirillaceae, Rhizobiaceae) collected at the particulate Mn oxide peak (winter Bering Sea Water) in the Canada Basin, displayed high relative abundances (Supporting Information Table SRD4) and were distributed among clades of cultured Mn oxidizers taxa (Supporting Information Fig. S5). This indicates that MnOB was likely present in the microbial communities of the Canada Basin at the time of sampling. Furthermore, several OTUs displaying high relative abundance (e.g., Phycisphaerales, Pirellulaceae, JTB38; Supporting Information Table SRD4) associated with high Mn oxide waters were found in samples from both, the Canada Basin and the other Arctic stations, and were identified in Mn oxide enriched environments (Supporting Information Fig. S5).

Particulate Mn biogeochemistry in light of microbial community structure

Altogether, these data provide strong support for the presence of specific microbial communities that are associated with high particulate Mn oxide samples across the Canadian Arctic Ocean, and highlight the Mn-oxidizing potential of the microbial communities associated with the peaks of particulate Mn characteristically found at intermediate depths of 50–300 m and near-bottom waters (Fig. 2). These waters have the potential to promote a significant increase in the relative abundance of MnOB within the microbial community, likely

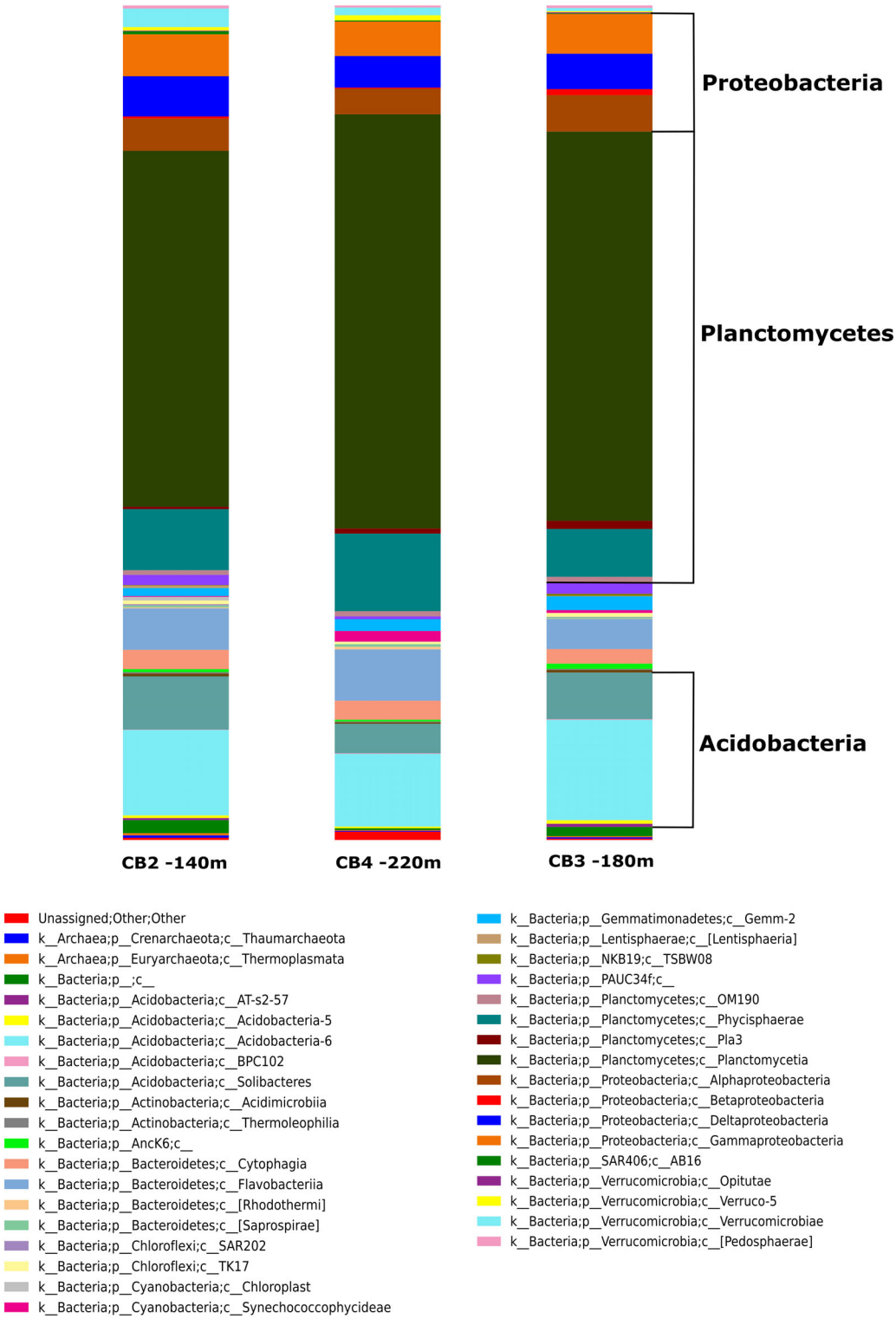

Fig. 4. Microbial community composition of three samples taken from the particulate Mn maximum in the Canada basin. 16S rRNA gene amplicon sequences were used to assess the taxonomic diversity, which is presented at either the class (c) or phylum (p) level for visualization. The top three phyla with the most relative abundance are labeled in bold in the figure.

enhancing the formation of Mn(III/IV) oxides. Subsurface waters in Southern Parry Channel (Stas. CAA4 and CAA7) and near-bottom waters in Baffin Bay slope region (Sta. BB1), where Mn oxides reach concentrations as high as ~ 4000–9000 pmol L^{-1} (Fig. 2), are characterized by a large relative abundance of microbes belonging to the following phyla (Fig. 3): Bacteroidota (f.Cryomorphaceae: X590041 and GT15.Ref.OTU23; GT15.Ref.OTU17.g.Saprospira), Proteobacteria (X328603.f.Colwelliaceae; X247681.f.Pisciric kettsiaceae; within the deltaproteobacteria class, the X315467.f.OM60 clade), Planctomycetota (f.Pirellulaceae: X543167, X3390990, and X4102516; o.Phycisphaerales: X1640197, X823094, and X813385), Nitrospinota (X921366.g.Nitrospina), Thaumarchaeota (g.Nitrosopumilus: X1005844 and X869040). Uncultured clades from the phyla Bacteroidota (OTUs: X826017.f.NS9), Planctomycetota (OTUs: X159828.o.CL500.15; GT15.Ref.OTU1.c.OM190; X564055.o.agg27), Proteobacteria (f.JTB38: X111722, X351152 and X593056), and Verrucomicrobiota (X32593.o.Arctic97B-4) are also largely abundant in subsurface waters in Parry Channel and near-bottom waters in Baffin Bay (Fig. 3). Likewise, in subsurface Arctic Water in Baffin Bay (Stas. BB1–BB3), where Mn oxides peaked (~ 1000–2000 pmol L^{-1}; Fig. 2), many of the above-mentioned OTUs (e.g., X315467.f.OM60; f.JTB38: X111722, X351152; f.Pirellulaceae: X543167, X3390990, and X4102516; X823094.o.Phycisphaerales) also dominate the microbial community (Fig. 3). Albeit differences in the sampling collection, the most abundant OTUs identified by 16S rRNA analysis in the winter Bering Sea Water Mn oxide maximum in the Canada Basin (~ 1600–5000 pmol L^{-1}; Fig. 2) are the same OTUs, or closely phylogenetically related, to those identified in the Arctic Water (Baffin Bay), subsurface waters in Southern Parry Channel and near-bottom waters in Baffin Bay slope region (Figs. 3, 4; Supporting Information Fig S5; Supporting Information Tables SRD2–SRD4).

The fact that we consistently observed higher relative abundance of the same OTUs—or phylogenetically related—in waters with high Mn oxides concentrations relative to those found in the remaining water column, and that those taxa have been also identified in other Mn oxide-dominated environments (Table 1) would suggest that in situ microbially-mediated Mn(II) oxidation is the driving mechanisms shaping the high Mn oxide features described across the Canadian Arctic Ocean.

Toward a mechanistic understanding of MnOB dynamics: Sedimentary microbe entrainment or environmental control

With the exception of the Labrador Sea, Mn oxides dominate particulate Mn distribution across the Canadian Arctic Ocean, a result of enhanced microbially-mediated authigenic oxidation, with prominent sharp Mn oxide peaks in the winter Bering Sea Water (Canada Basin), Arctic Water (Baffin Bay), southern Parry Channel subsurface waters, and near-bottom waters in Baffin Bay (Fig. 2). All these water masses have unique environmental conditions, such as being relatively deep, having elevated concentrations of dissolved Mn (~ 1 to > 10 nmol kg^{-1}; Colombo et al. 2020, 2022; Jensen et al. 2020), and having close interaction with the seafloor while transiting the Chukchi Sea (winter Bering Sea Water), the Canadian Arctic Archipelago (Southern Parry Channel subsurface waters and Arctic Water) and the sediment-water boundary layer (Baffin Bay near-bottom waters). Consequently, two different processes could be driving the highest relative abundances of putative MnOB in halocline waters and near-bottom Baffin Bay waters, and thus, the extent of authigenic Mn oxide precipitation: (1) Microbes are seeded from the benthic boundary layers into these waters, as a result of their close interaction with the seafloor, where microbial communities are taxonomically rich (Zinger et al. 2011; Walsh et al. 2016). A similar process has been described in hydrothermal plumes, where MnOB are seeded from surficial sediments and transported long distances (Dick et al. 2006; Fitzsimmons et al. 2017). (2) Distinct environmental conditions, such as low light, high oxygen, and dissolved Mn concentrations favor the abundance and diversity of MnOB populations in certain Canadian Arctic Ocean water masses (Sunda and Huntsman 1988; Moffett 1997; Zakharova et al. 2010). The microbial community composition data shed light on the predominance of these two processes. In the Canadian Arctic Ocean, favorable environmental conditions in the winter Bering Sea Water, Arctic Water, southern Parry Channel subsurface waters, and near-bottom waters in Baffin Bay most probably control the abundance of putative MnOB. The microbial relative abundance data, also known as compositional data (OTUs percent composition relative to the total OTUs present in the sample; Fig. 3), preclude the direct assessment of the microbial absolute abundance from different Canadian Arctic Ocean samples. However, putative MnOB is identified not only in high Mn oxide waters (large relative abundances) but also in waters that have not interacted with the seafloor recently (Colombo et al. 2019*b*) and have low Mn oxide concentrations, such as Baffin Bay deep waters (e.g., Fig. 3, samples BB2-304, BB2-1013, BB1-508). Similarly, putative MnOB are also found in Labrador Sea waters at low relative abundances (e.g., Fig. 3, samples LS2-304, LS2-506, LS2-1012, K1-509, K1-303, K1-608), where particulate Mn oxide concentrations were about an order of magnitude lower than in other Canadian Arctic Ocean stations (Fig. 2). This would indicate that MnOB are ubiquitously distributed across the Canadian Arctic Ocean (spatially and vertically; i.e., subsurface and deep waters), but they tend to dominate microbial communities in certain water masses that have favorable Mn oxide precipitation conditions. However, the lack of microbial community compositional data in the shallow Chukchi Shelf does not allow us to be conclusive.

Table 1. Selected particle-associated and/or putative Mn-oxidizing bacteria recovered at a high relative abundance where Mn oxide peaked in subsurface halocline waters and Baffin Bay near-bottom waters. The OTUs presented in this table, identified in the Canada Basin (Supporting Information Table SRD4) and the Canadian Arctic Archipelago, Baffin Bay, and the Labrador Sea (Supporting Information Tables SRD2 and SRD3) are displayed in Fig. 3 and Supporting Information Fig. S5.

Putative MnOB (OTUs)	Observations	Ref.
f.OM60: X315467, X817349, X885830	Phylogenetically related to representative cultured Mn(II)-oxidizing bacteria	Hansel (2017)
X159828.o.CL500-15	Particle-associated bacteria from the Southern Ocean	Milici et al. (2017)
GT15. referenceOTU1.c.OM190	Diverse OTUs within the Planctomycetota phylum have been isolated from deep Arctic Sea Fe hydroxide deposits	Storesund and Øvreås (2013)
f.JTB38: X111722, X351152	Top discriminating OTUs in SIMPER analysis; highly abundant in halocline waters	This study
f.Pirellulaceae: X543167, X3390990, X4102516, X4408871, X4376003, X4419144, X584647, ref. OTU4, ref. OTU5, ref. OTU7	Several OTUs within this family have been associated with biological Mn(II) oxidation, and are abundant in nitrifying and ammonia-oxidizing microbial consortia	Cao et al. (2015), Kellogg et al. (2016), Mohamed et al. (2010)
1,005,844.g.*Nitrosopumilus*	Several OTUs within this genus have been associated with biological Mn(II) oxidation, and are abundant in deep ocean ridge Fe–Mn environments and biofilms	Kato et al. (2017), Bergo et al. (2021)
o.Phycisphaerales: X823094, X837005, X813385, ref. OTU8, ref. OTU9, ref. OTU18	Several OTUs within this order have been associated with biological Mn(II) oxidation, and are abundant in Fe–Mn crust environments and biofilms in deep ocean ridge and sea coral settings	Bergo et al. (2021), Kellogg et al. (2016)
o.agg27: X564055, X726485	Particle-associated bacteria from the Southern Ocean and the Santa Barbara Channel	DeLong et al. (1993), Fuchsman et al. (2012)
GT15.ReferenceOTU17.g.Saprospira	Several OTUs within this genus have been associated with biological Mn(II) oxidation	Cao et al. (2015)
g. Moritella: X9017, X1133769	Phylogenetically related to representative cultured Mn(II)-oxidizing bacteria	Hansel (2017)

Among the environmental factors known to enhance MnOB diversity and abundance, we identify low light intensity (i.e., preventing photoinhibition) and high dissolved Mn concentrations as the key ones. Photoinhibition (i.e., physiological stress) of marine MnOB has been documented in laboratory incubation experiments, where Mn oxidation rates were significantly diminished when seawater was exposed to sunlight, to a much greater extent than that explained by photoreductive dissolution of Mn oxides alone (Sunda and Huntsman 1988; Francis et al. 2001). In our study, field microbial community composition data are consistent with laboratory experiments, as the discriminating OTUs (putative MnOB), which have large relative abundances in high Mn oxide waters, are virtually absent in most surface samples (depth < 50 m; Fig. 3; Supporting Information Fig. S6) where the lowest total particulate Mn and Mn oxide concentrations were measured (Fig. 2). Indeed, there is a shift of the microbial community structure from the deeper samples, dominated by taxa belonging to the phylum Planctomycetota and Proteobacteria, which include abundant OTUs that have been identified in Mn oxide enriched environments (OTUs: o.Phycisphaerales: X1640197, X823094, and X813385; f.Pirellulaceae: X543167, X3390990, and X4102516; X159828.o.CL500.15; GT15.Ref.OTU1.c.OM190; o.agg27: X726485 and X564055; etc.) to the shallower samples dominated by taxa belonging to Cyanobacteria and Bacteriodota phylum (Supporting Information Fig. S6). Detailed mechanisms underlying photoinhibition remain unknown, but the extremely low relative abundances of putative MnOB in surface waters in the Canadian Arctic Ocean would suggest sunlight directly affects microbial growth, and not only the rate of Mn oxide formation. In surface waters photoactivated reduction of Mn oxides by organic substances (Sunda et al. 1983; Sunda and Huntsman 1994) act in concert with MnOB photoinhibition, which contributes to the decrease of the particulate Mn pool and the accumulation of dissolved Mn (lower particulate Mn fraction; Fig. 2). Alleviation of photoinhibition in subsurface and deep waters itself does not ensure the proliferation of MnOB and associated enhanced bacterially-mediated Mn oxidation. Deep waters in the Canada Basin (depth > 300 m), Baffin Bay (depth > 200 m), and the Labrador Sea exhibit neither a large relative abundance of putative MnOB nor high Mn oxide concentrations (Figs. 2, 3), presumably a result of

dissolved Mn limitation. These deep waters, unlike subsurface halocline and Baffin Bay near-bottom waters, have subnanomolar levels of dissolved Mn (Colombo et al. 2020), a required micronutrient and reactant for MnOB (Moffett 1997; Zakharova et al. 2010; Cao et al. 2015).

Due to the small and low-density nature of Mn coatings on bacterial cells, small microbially-catalyzed Mn oxides (~ 0.5–1 μm) have been shown to be entrained and transported long distances (i.e., displaying no significant particle settling across isopycnals; Cowen and Silver 1984; Fitzsimmons et al. 2017). Accordingly, after begin formed, Mn oxides could be accumulated in halocline waters and be transported along their flow path, resulting in the Mn oxide peaks observed in subsurface halocline waters (Fig. 2). For example, in the Canada Basin, the winter Bering Sea Water takes one to 3 yr to travel from the Chukchi shelves to our sampled stations (Colombo et al. 2022), a time frame too short to allow small Mn oxides to settle out of the halocline water (from ~ 100 to 300 m), given their slow settling velocities (4–17 m yr^{-1} for 0.5–1 μm pure birnessite particles; Colombo et al. 2022). Note that bacterial Mn oxide capsule complexes have lower specific gravity than pure birnessite (Fitzsimmons et al. 2017; González-Santana et al. 2020). Thus, while transiting, Mn oxides are likely to accumulate in this layer. Hence, the halocline Mn oxide feature across the Canadian Arctic Ocean presumably reflects both (1) ongoing microbially-catalyzed oxidative precipitation, as long as there is no light and dissolved Mn concentrations are sufficient to sustain MnOB activity, and (2) an accumulated signature transported from slope regions where Mn oxides are formed once subsurface shelf waters with high dissolved Mn are advected to the ocean interior (Colombo et al. 2022).

It is worth noting that besides direct bacterially-mediated oxidation (i.e., MnOB activity), other oxidative pathways such as abiotic Mn oxidation by O_2 (Von Langen et al. 1997; Luther 2010) and indirect auto-catalytic and extracellular oxidation are probably influencing Mn oxide formation in halocline subsurface waters and near bottom Baffin Bay waters. Manganese oxide surfaces, especially the highly reactive phyllomanganate birnessite produced by microbes, accelerate the oxidation of Mn(II) by O_2 (auto-catalytic oxidation; Morgan 2005; Learman et al. 2011*b* and references therein). Similarly, indirect Mn(II) oxidation facilitated by microbial and fungal extracellular superoxide production has been shown in laboratory experiments (Learman et al. 2011*a*; Hansel et al. 2012; Jofré et al. 2021). These diverse (e.g., abiotic vs. biotic) and complex Mn oxidative pathways identified in laboratory experiments impose limitations when studying large-scale field studies. Hence, it is not possible to attribute unequivocally that the entire Mn oxide pool in these water masses is linked to direct enzymatic bacterially-mediated oxidation solely, and it is likely that the observed pool of Mn oxide is generated by a range of mechanisms rather than a single one. Notwithstanding, putative MnOB identified in this study, displaying high relative abundance where Mn oxides peaked, are most likely playing a preponderant role in shaping pMn distributions both directly by enzymatic activity catalyzing Mn(II) oxidation (Tebo et al. 2010; Hansel 2017; Yu and Leadbetter 2020) and indirectly by auto-catalytic and extracellular oxidation mechanisms, as described above.

Homogeneous abiotic Mn oxidation by O_2 (not including auto-catalytic surface reactions) cannot be ruled out as a plausible process; however, there is a substantial free energy barrier to the first one-electron oxidation rate-limiting step, Mn(II) + O_2 → Mn(III) + O_2^-, which start to occur only at pH values higher than 8 (Morgan 2005; Luther 2010). At pH values near those previously observed for Arctic Ocean surface waters (ca. < 8.0; Muth et al. 2022; pH data for our cruise is not available), in undersaturated Mn(II) solutions, the non-catalytic Mn oxidation reaction is extremely slow, exhibiting no Mn oxidation for 6 to 7 yr (Diem and Stumm 1984; Yu and Leadbetter 2020), resulting in rates that would be three to five orders of magnitude slower than bacterially-mediated Mn oxidation (Hastings and Emerson 1986; Von Langen et al. 1997). Considering the relatively short circulation time of halocline waters from the continental shelf-break and slope to the ocean interior—for instance, weeks to < 3 yr from the shelf-break to our sampled stations in the Canada Basin (Colombo et al. 2022)—homogeneous abiotic oxidation alone would not be a significant mechanism behind the rapid Mn oxide accumulation in these waters. Abiotic photochemical reactions generate reactive oxygen species, which can potentially oxidize Mn(II), but only if transient Mn(III) species are stabilized and hydrogen peroxide (H_2O_2) concentrations remain low, as H_2O_2 inhibits Mn(II) oxidation via the reduction of Mn(III) (Learman et al. 2013). Nonetheless, the colloidal nature of the poorly crystalline abiotically generated Mn oxides and their low ripening and aggregating behavior contrasts that of biotically derived Mn oxides, which rapidly precipitate and grow (Learman et al. 2013). Therefore, the extent and significance of Mn oxide formation through the abiotic superoxide oxidation pathway in subsurface halocline waters and bottom Baffin Bay waters is most probably negligible.

Finally, total particulate Mn distributions in Penny Strait (Sta. CAA9), Barrow Strait (Sta. CAA6), and northern Lancaster Sound (Sta. CAA1, close to Devon glaciers, and to a lesser extent Sta. CAA5) revealed an intriguing pattern: their particulate Mn concentrations were relatively lower than those of southern Parry Channel stations (Stas. CAA3, CAA4, and CAA7) and the lithogenic component dominated the particulate Mn pool (i.e., low Mn oxides; Fig. 2). The concentrations of dissolved Mn at the Stas. CAA1, CAA6, and CAA9 are well above subnanomolar levels (Colombo et al. 2020), and thereby, MnOB and Mn oxides should be higher below surface water, where photoinhibition is alleviated. This apparent inconsistency may be related to the presence of glacially-derived lithogenic particles and intense physical mixing in these regions, characteristics not found in the southern Parry Channel. Intense water column mixing is evidenced by the

near linearity of the θ–S profiles and the highest averaged diapycnal diffusivities and buoyancy fluxes reported in Penny Strait and Barrow Strait (Hughes et al. 2017; Colombo et al. 2021). Another observation that points toward stronger mixing regimes in Penny and Barrow straits, as well as northern Lancaster Sound, is the presence of sensible-heat polynyas—not present in southern Parry Channel—which are formed when heat from depth is brought to the surface by diapycnal mixing (Hannah et al. 2009). Tidal flow and the breaking of internal waves near Penny and Barrow strait sills and constrictions (Hannah et al. 2009; Hughes et al. 2017), the strong recirculation of Baffin Waters along northern Lancaster Sound shore (Hughes et al. 2017), along with buoyancy-driven upwelling induced by marine-terminating subglacial discharge in Devon Island are expected to enhance vertical mixing at the Stas. CAA1, CAA6, and CAA9 (and CAA5 to a lesser extent). Under such conditions, MnOB is mixed to a greater degree, presumably exposing these microbes to higher light levels, in Penny and Barrow straits and northern Lancaster Sound, compared with other stations in the CAA. In turn, strong mixing regimes at the Stas. CAA1, CAA5, CAA6, and CAA9 probably reduce the activity of MnOB (photoinhibition), and consequently, Mn oxide precipitation. Microbial community composition data support this argument since putative MnOB is present at high relative abundance where Mn oxides peaked (e.g., OTUs: X315467.f.OM60; f.JTB38: X111722, X351152; f.Pirellulaceae: X543167, X3390990, and X4102516; X823094.o.Phycisphaerales), display low relative abundances in subsurface waters at the Stas. CAA1, CAA5, and CAA6 (Fig. 3). Besides microbial photoinhibition, higher vertical mixing, and light exposure could potentially accelerate aggregation dynamics of Mn oxide particles and also enhance their reductive dissolution (Sunda and Huntsman 1988; Francis et al. 2001), having an additional detrimental effect on Mn oxide accumulation in Penny and Barrow straits and northern Lancaster Sound. The lack of seasonal data, absolute microbial abundance, and in situ mixing strength parameterization (e.g., eddy diffusivity) prevent us from being conclusive about this hypothesis, but recent work has documented the crucial role of strong physical mixing in influencing functional microbial communities and geochemical cycles, such as nitrogen speciation in coastal waters (Haas et al. 2021).

Concluding remarks

A comprehensive characterization of members of the microbial communities (on particulate material) associated with Mn oxidation has been accomplish by integrating particulate trace metal distributions along with microbial field data, lending additional support to the prominent role of MnOB in shaping particulate Mn cycling in the Canadian Arctic Ocean. The distributions of particulate Mn in the Canada Basin, the Canadian Arctic Archipelago, and Baffin Bay are distinguished by the dominance of Mn oxides (Fig. 2), attributed to microbially-mediated oxidation in the water column, especially in subsurface halocline waters and near-bottom Baffin Bay waters. In aforementioned water masses, putative MnOB display significantly higher relative abundances than those in the overlaying and underlying waters (Fig. 3). For instance, putative MnOB belonging to the phyla Bacteroidota, Planctomycetota, Proteobacteria, and Thaumarchaeota are abundant in water masses having elevated Mn oxide concentrations. Furthermore, numerous taxa identified in the Canada Basin halocline water, where non-lithogenic particulate Mn peaked, are phylogenetically related to known (cultured) MnOB (e.g., Rhodobacteraceae, Oceanospirillaceae, Rhizobiaceae). In addition, some of the putative MnOB OTUs (i.e., g. *Nitrosopumilus*, g.*Nitrospina*, o.*Phycisphaerales*, f. *Pirellulaceae*) identified in high Mn oxide waters belong to taxa known to oxidize nitrite or ammonium, suggesting that the N and Mn biogeochemical cycles might be linked, as proposed by Luther et al. (1997). The abundance of MnOB in Canadian Arctic Ocean waters may be primarily controlled by photoinhibition, as it has been demonstrated in laboratory studies; putative MnOB is virtually absent in surface water across the entire Canadian Arctic Ocean (Fig. 3). Below the surface, where photoinhibition is lessened or absent, the availability of dissolved Mn is anticipated to control MnOB dynamics. The highest relative abundances of putative MnOB within the Arctic Ocean are found in the winter Bering Sea Water (Canada Basin), Southern Parry Channel subsurface waters, Arctic Water (Baffin Bay), and near-bottom Baffin Bay waters, where Mn oxides concomitantly peaked. These water masses have unique environmental conditions: alleviation of photoinhibition and relatively high dissolved Mn concentrations, which allow MnOB to thrive, enhancing Mn oxidative processes at intermediate depths. In the Labrador Sea, particulate Mn concentrations were the lowest of all three basins, yielding balanced lithogenic/non-lithogenic contributions, presumably due to the scarcity of dissolved Mn (< 1 nmol kg^{-1} below subsurface waters), which may limit microbially-mediated Mn oxidation.

The presence of subsurface Mn oxide maxima, albeit with lower concentrations, has also been reported for other basins (e.g., Northeast Pacific, Western Subarctic Gyre, Eastern Pacific Zonal Transect; Lam et al. 2018; Lee et al. 2018; Sim 2018; Morton et al. 2019), which may suggest the proliferation of MnOB in subsurface waters is a global phenomenon. Coupling microbial community data with trace element analysis will greatly advance our knowledge about how MnOB and Mn cycling are interlinked and which are the key microbial taxa involved in Mn oxidation.

Data availability statement

The particulate Mn data along with ancillary data reported in this study is available in the public repositories: the GEOTRACES Intermediate Data Product 2021 via the British Oceanographic Data Centre (https://www.bodc.ac.uk/geotraces/data/idp2021/). The 16S amplicon reads and the representative

OTU sequences obtained from the subsequent processing are in the process of being submitted to the NCBI database. In addition, all the data presented in this paper is also available in the Research Data Electronic Annex. Supporting Information Tables S1 and S2 and Figs. S1–S6 are included in the Supporting Information.

References

Aksenov, Y., V. V. Ivanov, A. J. G. Nurser, S. Bacon, I. V. Polyakov, A. C. Coward, A. C. Naveira-Garabato, and A. Beszczynska-Moeller. 2011. The arctic circumpolar boundary current. J. Geophys. Res.: Oceans **116**: 1–28. doi:10.1029/2010JC006637

Bergo, N. M., A. G. Bendia, J. C. N. Ferreira, B. Murton, F. P. Brandini, and D. V. H. Pellizari. 2021. Microbial diversity of deep-sea ferromanganese crust field in the Rio Grande Rise, southwestern Atlantic Ocean. Microb. Ecol. **82**: 344–355. doi:10.1101/2020.06.13.150011

Cao, L. T. T., H. Kodera, K. Abe, H. Imachi, Y. Aoi, T. Kindaichi, N. Ozaki, and A. Ohashi. 2015. Biological oxidation of Mn(II) coupled with nitrification for removal and recovery of minor metals by downflow hanging sponge reactor. Water Res. **68**: 545–553. doi:10.1016/j.watres.2014.10.002

Caporaso, J. G., and others. 2010. QIIME allows analysis of high-throughput community sequencing data. Nat. Methods **7**: 335–336. doi:10.1038/nmeth.f.303

Clarke, K. R., and R. N. Gorley. 2006. PRIMER v6: User manual/tutoria. PRIMER-E.

Colombo, M., K. A. Brown, J. De Vera, B. A. Bergquist, and K. J. Orians. 2019*a*. Trace metal geochemistry of remote rivers in the Canadian Arctic archipelago. Chem. Geol. **525**: 479–491. doi:10.1016/j.chemgeo.2019.08.006

Colombo, M., B. Rogalla, P. G. Myers, S. E. Allen, and K. J. Orians. 2019*b*. Tracing dissolved lead sources in the Canadian Arctic: Insights from the Canadian GEOTRACES program. ACS Earth Space Chem. **3**: 1302–1314. doi:10.1021/acsearthspacechem.9b00083

Colombo, M., S. L. Jackson, J. T. Cullen, and K. J. Orians. 2020. Dissolved iron and manganese in the Canadian Arctic Ocean: On the biogeochemical processes controlling their distributions. Geochim. Cosmochim. Acta **277**: 150–174. doi:10.1016/j.gca.2020.03.012

Colombo, M., B. Rogalla, J. Li, S. E. Allen, K. J. Orians, and M. T. Maldonado. 2021. Canadian Arctic archipelago shelf-ocean interactions: A major iron source to Pacific derived waters transiting to the Atlantic. Glob. Biogeochem. Cycles **35**: e2021GB007058. doi:10.1029/2021GB007058

Colombo, M., J. Li, B. Rogalla, S. E. Allen, and M. T. Maldonado. 2022. Particulate trace element distributions along the Canadian Arctic GEOTRACES section: Shelf-water interactions, advective transport and contrasting biological production. Geochim. Cosmochim. Acta **323**: 183–201. doi:10.1016/j.gca.2022.02.013

Comeau, A. M., G. M. Douglas, and M. G. I. Langille. 2017. Microbiome helper: A custom and streamlined workflow for microbiome research. mSystems **2**: e00127-16. doi:10.1128/mSystems.00127-16

Cowen, J. P., and M. W. Silver. 1984. The association of iron and manganese with bacteria on marine macroparticulate material. Science **224**: 1340–1342. doi:10.1126/science.224.4655.1340

DeLong, E. F., D. G. Franks, and A. L. Alldredge. 1993. Phylogenetic diversity of aggregate-attached vs. free-living marine bacterial assemblages. Limnol. Oceanogr. **38**: 924–934. doi:10.4319/lo.1993.38.5.0924

DeSantis, T. Z., and others. 2006. Greengenes, a chimera-checked 16S rRNA gene database and workbench compatible with ARB. Appl. Environ. Microbiol. **72**: 5069–5072. doi:10.1128/AEM.03006-05

Dick, G. J., Y. E. Lee, and B. M. Tebo. 2006. Manganese(II)-oxidizing *Bacillus* spores in Guaymas Basin hydrothermal sediments and plumes. Appl. Environ. Microbiol. **72**: 3184–3190. doi:10.1128/AEM.72.5.3184-3190.2006

Diem, D., and W. Stumm. 1984. Is dissolved Mn^{2+} being oxidized by O_2 in absence of Mn-bacteria or surface catalysts? Geochim. Cosmochim. Acta **48**: 1571–1573. doi:10.1016/0016-7037(84)90413-7

Ehrlich, H. L., and D. K. Newman [eds.]. 2008. Geomicrobiology, 5th ed. CRC Press.

Faust, K., and J. Raes. 2016. CoNet app: Inference of biological association networks using Cytoscape. F1000Research **5**: 1519. doi:10.12688/f1000research.9050.2

Fitzsimmons, J. N., S. G. John, C. M. Marsay, C. L. Hoffman, S. L. Nicholas, B. M. Toner, C. R. German, and R. M. Sherrell. 2017. Iron persistence in a distal hydrothermal plume supported by dissolved-particulate exchange. Nat. Geosci. **10**: 195–201. doi:10.1038/ngeo2900

Francis, C. A., E. M. Co, and B. M. Tebo. 2001. Enzymatic manganese(II) oxidation by a marine α-proteobacterium. Appl. Environ. Microbiol. **67**: 4024–4029. doi:10.1128/AEM.67.9.4024-4029.2001

Fuchsman, C. A., J. T. Staley, B. B. Oakley, J. B. Kirkpatrick, and J. W. Murray. 2012. Free-living and aggregate-associated planctomycetes in the Black Sea. FEMS Microbiol. Ecol. **80**: 402–416. doi:10.1111/j.1574-6941.2012.01306.x

GEOTRACES Intermediate Data Product Group. 2021. The GEOTRACES Intermediate Data Product 2021 (IDP2021).

González-Santana, D., and others. 2020. Processes driving iron and manganese dispersal from the TAG hydrothermal plume (mid-Atlantic ridge): Results from a GEOTRACES process study. Front. Mar. Sci. **7**: 568. doi:10.3389/fmars.2020.00568

Granger, J., D. M. Sigman, J. Gagnon, J.-É. Tremblay, and A. Mucci. 2018. On the properties of the Arctic halocline and

deep water masses of the Canada Basin from nitrate isotope ratios. J. Geophys. Res.: Oceans **123**: 5443–5458. doi:10.1029/2018JC014110

Haas, S., B. M. Robicheau, S. Rakshit, J. Tolman, C. K. Algar, J. LaRoche, and D. W. R. Wallace. 2021. Physical mixing in coastal waters controls and decouples nitrification via biomass dilution. Proc. Natl. Acad. Sci. USA **118**: e2004877118. doi:10.1073/pnas.2004877118

Hannah, C. G., F. Dupont, and M. Dunphy. 2009. Polynyas and tidal currents in the Canadian Arctic archipelago. Arctic **62**: 83–95. doi:10.14430/arctic115

Hansel, C. M. 2017. Manganese in marine microbiology, p. 37–83. *In* R. K. Poole [ed.], Advances in microbial physiology. Elsevier. doi:10.1016/bs.ampbs.2017.01.005

Hansel, C. M., C. A. Zeiner, C. M. Santelli, and S. M. Webb. 2012. Mn(II) oxidation by an ascomycete fungus is linked to superoxide production during asexual reproduction. Proc. Natl. Acad. Sci. USA **109**: 12621–12625. doi:10.1073/pnas.1203885109

Hastings, D., and S. Emerson. 1986. Oxidation of manganese by spores of a marine bacillus: Kinetic and thermodynamic considerations. Geochim. Cosmochim. Acta **50**: 1819–1824. doi:10.1016/0016-7037(86)90141-9

Hill, V. J., P. A. Matrai, E. Olson, S. Suttles, M. Steele, L. A. Codispoti, and R. C. Zimmerman. 2013. Synthesis of integrated primary production in the Arctic Ocean: II. In situ and remotely sensed estimates. Prog. Oceanogr. **110**: 107–125. doi:10.1016/j.pocean.2012.11.005

Hughes, K. G., J. M. Klymak, X. Hu, and P. G. Myers. 2017. Water mass modification and mixing rates in a 1/12° simulation of the Canadian Arctic Archipelago. J. Geophys. Res.: Oceans **122**: 803–820. doi:10.1002/2016JC012235

Jensen, L. T., and others. 2020. A comparison of marine Fe and Mn cycling: U.S. GEOTRACES GN01 Western Arctic case study. Geochim. Cosmochim. Acta **288**: 138–160. doi:10.1016/j.gca.2020.08.006

Jofré, I., F. Matus, D. Mendoza, F. Nájera, and C. Merino. 2021. Manganese-oxidizing antarctic bacteria (Mn-Oxb) release reactive oxygen species (ROS) as secondary Mn(II) oxidation mechanisms to avoid toxicity. Biology **10**: 1004. doi:10.3390/biology10101004

Kato, S., and others. 2017. Biotic manganese oxidation coupled with methane oxidation using a continuous-flow bioreactor system under marine conditions. Water Sci. Technol. **76**: 1781–1795. doi:10.2166/wst.2017.365

Kellogg, C. T. E., and J. W. Deming. 2009. Comparison of free-living, suspended particle, and aggregate-associated bacterial and archaeal communities in the Laptev Sea. Aquat. Microb. Ecol. **57**: 1–18. doi:10.3354/ame01317

Kellogg, C. A., S. W. Ross, and S. D. Brooke. 2016. Bacterial community diversity of the deep-sea octocoral *Paramuricea placomus*. PeerJ **4**: e2529. doi:10.7717/peerj.2529

Kondo, Y., H. Obata, N. Hioki, A. Ooki, S. Nishino, T. Kikuchi, and K. Kuma. 2016. Transport of trace metals (Mn, Fe, Ni, Zn and Cd) in the western Arctic Ocean (Chukchi Sea and Canada Basin) in late summer 2012. Deep-Sea Res. I: Oceanogr. Res. Pap. **116**: 236–252. doi:10.1016/j.dsr.2016.08.010

Lam, P. J., D. C. Ohnemus, and M. E. Auro. 2015. Size-fractionated major particle composition and concentrations from the US GEOTRACES North Atlantic Zonal Transect. Deep-Sea Res. II: Top. Stud. Oceanogr. **116**: 303–320. doi:10.1016/j.dsr2.2014.11.020

Lam, P. J., J. M. Lee, M. I. Heller, S. Mehic, Y. Xiang, and N. R. Bates. 2018. Size-fractionated distributions of suspended particle concentration and major phase composition from the U.S. GEOTRACES Eastern Pacific Zonal Transect (GP16). Mar. Chem. **201**: 90–107. doi:10.1016/j.marchem.2017.08.013

Learman, D. R., B. M. Voelker, A. I. Vazquez-Rodriguez, and C. M. Hansel. 2011*a*. Formation of manganese oxides by bacterially generated superoxide. Nat. Geosci. **4**: 95–98. doi:10.1038/ngeo1055

Learman, D. R., S. D. Wankel, S. M. Webb, N. Martinez, A. S. Madden, and C. M. Hansel. 2011*b*. Coupled biotic-abiotic Mn(II) oxidation pathway mediates the formation and structural evolution of biogenic Mn oxides. Geochim. Cosmochim. Acta **75**: 6048–6063. doi:10.1016/j.gca.2011.07.026

Learman, D. R., B. M. Voelker, A. S. Madden, and C. M. Hansel. 2013. Constraints on superoxide mediated formation of manganese oxides. Front. Microbiol. **4**: 262. doi:10.3389/fmicb.2013.00262

Lee, J. M., M. I. Heller, and P. J. Lam. 2018. Size distribution of particulate trace elements in the U.S. GEOTRACES Eastern Pacific Zonal Transect (GP16). Mar. Chem. **201**: 108–123. doi:10.1016/j.marchem.2017.09.006

Lehmann, N., M. Kienast, J. Granger, and J. Tremblay. 2022. Physical and biogeochemical influences on nutrients through the Canadian Arctic Archipelago: Insights from nitrate isotope ratios. J. Geophys. Res.: Oceans **127**: e2021JC018179. doi:10.1029/2021JC018179

Luther, G. W. 2010. The role of one- and two-electron transfer reactions in forming thermodynamically unstable intermediates as barriers in multi-electron redox reactions. Aquat. Geochem. **16**: 395–420. doi:10.1007/s10498-009-9082-3

Luther, G. W., B. Sundby, B. L. Lewis, P. J. Brendel, and N. Silverberg. 1997. Interactions of manganese with the nitrogen cycle: Alternative pathways to dinitrogen. Geochim. Cosmochim. Acta **61**: 4043–4052. doi:10.1016/S0016-7037(97)00239-1

Mahowald, N. M., D. S. Hamilton, K. R. M. Mackey, J. K. Moore, A. R. Baker, R. A. Scanza, and Y. Zhang. 2018. Aerosol trace metal leaching and impacts on marine microorganisms. Nat. Commun. **9**: 2614. doi:10.1038/s41467-018-04970-7

Marsay, C. M., and others. 2018. Dissolved and particulate trace elements in late summer Arctic melt ponds. Mar. Chem. **204**: 70–85. doi:10.1016/j.marchem.2018.06.002

Middag, R., H. J. W. de Baar, P. Laan, and M. B. Klunder. 2011. Fluvial and hydrothermal input of manganese into the Arctic Ocean. Geochim. Cosmochim. Acta **75**: 2393–2408. doi:10.1016/j.gca.2011.02.011

Middag, R., H. J. W. de Baar, M. B. Klunder, and P. Laan. 2013. Fluxes of dissolved aluminum and manganese to the Weddell Sea and indications for manganese co-limitation. Limnol. Oceanogr. **58**: 287–300. doi:10.4319/lo.2013.58.1.0287

Milici, M., and others. 2017. Diversity and community composition of particle-associated and free-living bacteria in mesopelagic and bathypelagic Southern Ocean water masses: Evidence of dispersal limitation in the Bransfield Strait. Limnol. Oceanogr. **62**: 1080–1095. doi:10.1002/lno.10487

Moffett, J. W. 1997. The importance of microbial Mn oxidation in the upper ocean: A comparison of the Sargasso Sea and equatorial Pacific. Deep-Sea Res. I: Oceanogr. Res. Pap. **44**: 1277–1291. doi:10.1016/S0967-0637(97)00032-0

Mohamed, N. M., K. Saito, Y. Tal, and R. T. Hill. 2010. Diversity of aerobic and anaerobic ammonia-oxidizing bacteria in marine sponges. ISME J. **4**: 38–48. doi:10.1038/ismej.2009.84

Morel, F. M. M. M., A. J. Milligan, and M. A. Saito. 2013. Marine bioinorganic chemistry: The role of trace metals in the oceanic cycles of major nutrients, p. 113–143. *In* H. D. Holland and K. K. Turekian [eds.], Treatise on geochemistry, v. **6**, 2nd ed. Elsevier. doi:10.1016/B0-08-043751-6/06108-9

Morgan, J. J. 2005. Kinetics of reaction between O_2 and Mn(II) species in aqueous solutions. Geochim. Cosmochim. Acta **69**: 35–48. doi:10.1016/j.gca.2004.06.013

Morton, P. L., and others. 2019. Shelf inputs and lateral transport of Mn, Co, and Ce in the western north pacific ocean. Front. Mar. Sci. **6**: 591. doi:10.3389/fmars.2019.00591

Muth, A. F., A. L. Kelley, and K. H. Dunton. 2022. High-frequency pH time series reveals pronounced seasonality in Arctic coastal waters. Limnol. Oceanogr. **67**: 1429–1442. doi:10.1002/lno.12080

Ohnemus, D. C., M. E. Auro, R. M. Sherrell, M. Lagerström, P. L. Morton, B. S. Twining, S. Rauschenberg, and P. J. Lam. 2014. Laboratory intercomparison of marine particulate digestions including piranha: A novel chemical method for dissolution of polyethersulfone filters. Limnol. Oceanogr.: Methods **12**: 530–547. doi:10.4319/lom.2014.12.530

Oldham, V. E., A. Mucci, B. M. Tebo, and G. W. Luther. 2017. Soluble Mn(III)–L complexes are abundant in oxygenated waters and stabilized by humic ligands. Geochim. Cosmochim. Acta **199**: 238–246. doi:10.1016/j.gca.2016.11.043

Pakhomova, S. V., A. G. Rozanov, and E. V. Yakushev. 2009. Dissolved and particulate forms of iron and manganese in the redox zone of the Black Sea. Oceanology **49**: 773–787. doi:10.1134/S0001437009060046

Parada, A. E., D. M. Needham, and J. A. Fuhrman. 2016. Every base matters: Assessing small subunit rRNA primers for marine microbiomes with mock communities, time series and global field samples. Environ. Microbiol. **18**: 1403–1414. doi:10.1111/1462-2920.13023

Pausch, F., K. Bischof, and S. Trimborn. 2019. Iron and manganese co-limit growth of the Southern Ocean diatom *Chaetoceros debilis*. PloS One **14**: e0221959. doi:10.1371/journal.pone.0221959

Rogalla, B., S. E. Allen, M. Colombo, P. G. Myers, and K. J. Orians. 2022. Sediments in sea ice drive the Canada Basin surface Mn maximum: Insights from an Arctic Mn Ocean model. Glob. Biogeochem. Cycles **36**: e2022GB007320. doi:10.1029/2022GB007320

Rognes, T., T. Flouri, B. Nichols, C. Quince, and F. Mahé. 2016. VSEARCH: A versatile open source tool for metagenomics. PeerJ **4**: e2584. doi:10.7717/peerj.2584

Rudnick, R. L., and S. Gao. 2013. Composition of the continental crust, p. 1–64. *In* H. D. Holland and K. K. Turekian [eds.], Treatise on geochemistry, v. **3**, 2nd ed. Elsevier. doi:10.1016/B0-08-043751-6/03016-4

Shannon, P., and others. 2003. Cytoscape: A software environment for integrated models of biomolecular interaction networks. Genome Res. **13**: 2498–2504. doi:10.1101/gr.1239303

Sim, N. 2018. Biogeochemical cycling of dissolved and particulate manganese in the Northeast Pacific and Canadian western Arctic. Ph.D. thesis. Univ. of British Columbia.

Storesund, J. E., and L. Øvreås. 2013. Diversity of *Planctomycetes* in iron-hydroxide deposits from the Arctic Mid Ocean Ridge (AMOR) and description of *Bythopirellula goksoyri* gen. nov., sp. nov., a novel *Planctomycete* from deep sea iron-hydroxide deposits. Antonie van Leeuwenhoek **104**: 569–584. doi:10.1007/s10482-013-0019-x

Sunda, W. G., and S. A. Huntsman. 1988. Effect of sunlight on redox cycles of manganese in the southwestern Sargasso Sea. Deep-Sea Res. A: Oceanogr. Res. Pap. **35**: 1297–1317. doi:10.1016/0198-0149(88)90084-2

Sunda, W. G., and S. A. Huntsman. 1994. Photoreduction of manganese oxides in seawater. Mar. Chem. **46**: 133–152. doi:10.1016/0304-4203(94)90051-5

Sunda, W. G., S. A. Huntsman, and G. R. Harvey. 1983. Photoreduction of manganese oxides in seawater and its geochemical and biological implications. Nature **301**: 234–236. doi:10.1038/301234a0

Tebo, B. M., J. R. Bargar, B. G. Clement, G. J. Dick, K. J. Murray, D. Parker, R. Verity, and S. M. Webb. 2004. Biogenic manganese oxides: Properties and mechanisms of formation. Annu. Rev. Earth Planet. Sci. **32**: 287–328. doi:10.1146/annurev.earth.32.101802.120213

Tebo, B. M., K. Geszvain, and S. W. Lee. 2010. The molecular geomicrobiology of bacterial manganese(II) oxidation, p. 285–308. *In* L. Barton, M. Mandl, and A. Loy [eds.], Geomicrobiology: Molecular and environmental perspective. Springer. doi:10.1007/978-90-481-9204-5_13

Twining, B. S., S. Rauschenberg, P. L. Morton, and S. Vogt. 2015. Metal contents of phytoplankton and labile particulate material in the North Atlantic Ocean. Prog. Oceanogr. **137**: 261–283. doi:10.1016/j.pocean.2015.07.001

van Hulten, M., R. Middag, J.-C. Dutay, H. de Baar, M. Roy-Barman, M. Gehlen, A. Tagliabue, and A. Sterl. 2017. Manganese in the West Atlantic Ocean in the context of the first global ocean circulation model of manganese. Biogeosciences **14**: 1123–1152. doi:10.5194/bg-14-1123-2017

Varela, D. E., D. W. Crawford, I. A. Wrohan, S. N. Wyatt, and E. C. Carmack. 2013. Pelagic primary productivity and upper ocean nutrient dynamics across subarctic and Arctic seas. J. Geophys. Res.: Oceans **118**: 7132–7152. doi:10.1002/2013JC009211

Vieira, L. H., E. P. Achterberg, J. Scholten, A. J. Beck, V. Liebetrau, M. M. Mills, and K. R. Arrigo. 2019. Benthic fluxes of trace metals in the Chukchi Sea and their transport into the Arctic Ocean. Mar. Chem. **208**: 43–55. doi:10.1016/j.marchem.2018.11.001

von Langen, P. J., K. S. Johnson, K. H. Coale, and V. A. Elrod. 1997. Oxidation kinetics of manganese (II) in sea water at nanomolar concentrations. Geochim. Cosmochim. Acta **61**: 4945–4954. doi:10.1016/S0016-7037(97)00355-4

Walsh, E. A., J. B. Kirkpatrick, S. D. Rutherford, D. C. Smith, M. Sogin, and S. D'Hondt. 2016. Bacterial diversity and community composition from seasurface to subseafloor. ISME J. **10**: 979–989. doi:10.1038/ismej.2015.175

Wang, D., H. Lin, Q. Ma, Y. Bai, and J. Qu. 2021. Manganese oxides in *Phragmites* rhizosphere accelerates ammonia oxidation in constructed wetlands. Water Res. **205**: 117688. doi:10.1016/j.watres.2021.117688

Webb, S. M., G. J. Dick, J. R. Bargar, and B. M. Tebo. 2005. Evidence for the presence of Mn(III) intermediates in the bacterial oxidation of Mn(II). Proc. Natl. Acad. Sci. USA **102**: 5558–5563. doi:10.1073/pnas.0409119102

Wright, M. H., K. Geszvain, V. E. Oldham, G. W. Luther, and B. M. Tebo. 2018. Oxidative formation and removal of complexed Mn(III) by *Pseudomonas* species. Front. Microbiol. **9**: 560. doi:10.3389/fmicb.2018.00560

Xiang, Y., and P. J. Lam. 2020. Size-fractionated compositions of marine suspended particles in the Western Arctic Ocean: Lateral and vertical sources. J. Geophys. Res.: Oceans **125**: e2020JC016144. doi:10.1029/2020JC016144

Yu, H., and J. R. Leadbetter. 2020. Bacterial chemolithoautotrophy via manganese oxidation. Nature **583**: 453–458. doi:10.1038/s41586-020-2468-5

Zakharova, Y. R., V. V. Parfenova, L. Z. Granina, O. S. Kravchenko, and T. I. Zemskaya. 2010. Distribution of iron- and manganese-oxidizing bacteria in the bottom sediments of Lake Baikal. Inland Water Biol. **3**: 313–321. doi:10.1134/S1995082910040036

Zhang, H., H. Wu, G. Wang, W. Xiang, and Y. Wen. 2013. Prokaryote diversity in the surface sediment of northern South China Sea. Wei Sheng Wu Xue Bao **53**: 915–926.

Zhang, J., K. Kobert, T. Flouri, and A. Stamatakis. 2014. PEAR: A fast and accurate Illumina Paired-End reAd mergeR. Bioinformatics **30**: 614–620. doi:10.1093/bioinformatics/btt593

Zinger, L., and others. 2011. Global patterns of bacterial beta-diversity in seafloor and seawater ecosystems. PloS One **6**: e24570. doi:10.1371/journal.pone.0024570

Zorz, J., C. Willis, A. M. Comeau, M. G. I. Langille, C. L. Johnson, W. K. W. Li, and J. LaRoche. 2019. Drivers of regional bacterial community structure and diversity in the Northwest Atlantic Ocean. Front. Microbiol. **10**: 281. doi:10.3389/fmicb.2019.00281

Acknowledgments

This work was supported by the Natural Sciences and Engineering Research Council of Canada with the grant NSERC-CCAR, the grant NSERC DG to J.L.R. and a NSERC Post-Doctoral fellowship award to M.C., and the Northern Scientific Training Program. The authors thank the captain and crew of the CCGS Amundsen as well as Chief Scientist Roger Francois, PI Jay Cullen and Kristin Orians, and the trace metal rosette group (Sarah Jackson, Priyanka Chandan, Kang Wang, Kathleen Munson, David Semeniuk, Dave Janssen, Rowan Fox, and Kathryn Purdon) for their assistance in sample collection. The Pacific Centre for Isotopic and Geochemical Research and its staff are thanked for assistance with sample analyses. We also thank three reviewers for their meaningful comments and suggestions.

Conflict of Interest

None declared.

Submitted 17 June 2022
Revised 29 October 2022
Accepted 05 July 2023

Associate editor: Osvaldo Ulloa